Eur J Nucl Med Mol Imaging
DOI 10.1007/s00259-015-3232-1

ORIGINAL ARTICLE

Preclinical and first clinical experience with the gastrin-releasing peptide receptor-antagonist [^{68}Ga]SB3 and PET/CT

Theodosia Maina[1] · Hendrik Bergsma[2] · Harshad R. Kulkarni[4] · Dirk Mueller[4] · David Charalambidis[1] · Eric P. Krenning[2] · Berthold A. Nock[1] · Marion de Jong[2,3] · Richard P. Baum[4]

Received: 14 July 2015 / Accepted: 15 October 2015

Abstract
Purpose Gastrin-releasing peptide receptors (GRPR) represent attractive targets for tumor diagnosis and therapy because of their overexpression in major human cancers. Internalizing GRPR agonists were initially proposed for prolonged lesion retention, but a shift of paradigm to GRPR antagonists has recently been made. Surprisingly, radioantagonists, such as [^{99m}Tc]DB1 (^{99m}Tc-N$_4$′-DPhe^6,Leu-NHEt^{13}]BBN(6–13)), displayed better pharmacokinetics than radioagonists, in addition to their higher inherent biosafety. We introduce here [^{68}Ga]SB3, a [^{99m}Tc]DB1 mimic-carrying, instead of the ^{99m}Tc-binding tetraamine, the chelator DOTA for labeling with the PET radiometal ^{68}Ga.
Methods Competition binding assays of SB3 and [^{nat}Ga]SB3 were conducted against [^{125}I-Tyr^4]BBN in PC-3 cell membranes. Blood samples collected 5 min postinjection (pi) of the [^{67}Ga]SB3 surrogate in mice were analyzed using high-performance liquid chromatography (HPLC) for degradation products. Likewise, biodistribution was performed after injection of [^{67}Ga]SB3 (37 kBq, 100 μL, 10 pmol peptide) in severe combined immunodeficiency (SCID) mice bearing PC-3 xenografts. Eventually, [^{68}Ga]SB3 (283±91 MBq, 23±7 nmol) was injected into 17 patients with breast (8) and prostate (9) cancer. All patients had disseminated disease and had received previous therapies. PET/CT fusion images were acquired 60–115 min pi.
Results SB3 and [^{nat}Ga]SB3 bound to the human GRPR with high affinity (IC_{50}: 4.6±0.5 nM and 1.5±0.3 nM, respectively). [^{67}Ga]SB3 displayed good in vivo stability (>85 % intact at 5 min pi). [^{67}Ga]SB3 showed high, GRPR-specific and prolonged retention in PC-3 xenografts (33.1±3.9%ID/g at 1 h pi – 27.0±0.9%ID/g at 24 h pi), but much faster clearance from the GRPR-rich pancreas (≈160%ID/g at 1 h pi to <17%ID/g at 24 h pi) in mice. In patients, [^{68}Ga]SB3 elicited no adverse effects and clearly visualized cancer lesions. Thus, 4 out of 8 (50 %) breast cancer and 5 out of 9 (55 %) prostate cancer patients showed pathological uptake on PET/CT with [^{68}Ga]SB3.
Conclusion [^{67}Ga]SB3 showed excellent pharmacokinetics in PC-3 tumor-bearing mice, while [^{68}Ga]SB3 PET/CT visualized lesions in about 50 % of patients with advanced and metastasized prostate and breast cancer. We expect imaging with [^{68}Ga]SB3 to be superior in patients with primary breast or prostate cancer.

Keywords PET/CT tumor imaging · ^{68}Ga radiotracer · Gastrin-releasing peptide receptor antagonist · Prostate cancer · Breast cancer

Theodosia Maina and Hendrik Bergsma contributed equally to this work

Electronic supplementary material The online version of this article (doi:10.1007/s00259-015-3232-1) contains supplementary material, which is available to authorized users

✉ Theodosia Maina
maina_thea@hotmail.com

[1] Molecular Radiopharmacy, INRASTES, NCSR "Demokritos", Ag. Paraskevi Attikis, 15310 Athens, Greece

[2] Department of Nuclear Medicine, Erasmus MC, Rotterdam, The Netherlands

[3] Department of Radiology, Erasmus MC, Rotterdam, The Netherlands

[4] Molecular Radiotherapy and Molecular Imaging, Zentralklinik, Bad Berka, Germany

Introduction

Prostate (PC) and breast cancer (BC) rank first in incidence among men and women diagnosed with cancer in Western

Published online: 02 December 2015

countries and are linked to considerable morbidity and mortality in the metastatic stages of the disease [1, 2]. Accordingly, the non-invasive and reliable diagnosis and staging of these cancers remain compelling medical requirements. This is reflected in the high number of inconclusive biopsies, which are associated with much patient discomfort and anxiety, and with an increase in healthcare costs [3, 4]. On the other hand, conventional imaging techniques, such as MRI, CT, ultrasound, or even established nuclear medicine procedures (e.g., ^{18}FDG/PET) remain of limited diagnostic value because of their low specificity [5–8].

In this respect, receptor-targeted tumor imaging may represent an attractive alternative for diagnosing primary and/or disseminated disease with high specificity and sensitivity. This approach holds great promise in cases of PC and BC, owing to the high density expression of the gastrin-releasing peptide receptor (GRPR) target in pathological lesions. In particular, high GRPR expression has been documented in primary and well-differentiated PC (85–100 %), which, however, drops (50 %) in androgen-refractory bone metastases [9–13]. GRPR is also expressed in primary BC (>60 %), whereas all metastases originating from GRPR-positive primaries retain high levels of receptor expression [14–16].

Originally, radiolabeled analogs of the frog tetradecapeptide bombesin (BBN) have been developed for the in vivo targeting of GRPR-positive tumor sites, mainly owing to their ability to internalize rapidly and massively into cancer cells [17, 18]. At that time, internalization was considered essential for prolonged lesion retention, which would eventually translate into greater diagnostic sensitivity and therapeutic efficacy. However, this rationale has been challenged by accumulating evidence on the unexpectedly superior performance of radiolabeled GRPR antagonists in visualizing GRPR-positive tumors in vivo versus their agonist-based counterparts [19, 20]. Thus, the radioantagonist [^{99m}Tc]DB1 has displayed higher uptake and retention in GRPR-expressing tumors in combination with a much faster background clearance (including the GRPR-rich pancreas) than the radioagonist [^{99m}Tc]DB4 [19]. A further significant advantage of radioantagonists is their greater inherent biosafety. In contrast to agonists, GRPR antagonists do not elicit pharmacological effects after receptor binding and are consequently better tolerated after intravenous (iv) injection to patients [21].

In the current work, we introduce the [^{99m}Tc]DB1 mimic [^{68}Ga]SB3 (Fig. 1), whereby the ^{99m}Tc-binding acyclic tetraamine unit has been replaced by the chelator DOTA to allow labeling with the PET radiometal ^{68}Ga. The new PET tracer has been characterized in GRPR-positive cells and animal models using the [^{67}Ga]SB3 surrogate. Furthermore, a first-in-man clinical evaluation of [^{68}Ga]SB3 has been performed in a small number of patients with recurrent PC or BC employing PET/CT.

Materials and methods

SB3 and [$^{67/68}$Ga]SB3

The DOTA-conjugated GRPR antagonist SB3 (DOTA-*p*-aminomethylaniline-diglycolic acid-DPhe-Gln-Trp-Ala-Val-Gly-His-Leu-NHEt) was obtained from PiChem and labeled with ^{67}Ga or ^{68}Ga, as detailed in the Supplementary material; quality control of the radiolabeled product (Fig. 1) is also presented therein.

In vitro assays

Human androgen-independent prostate adenocarcinoma PC-3 cells (LGC Promochem) endogenously expressing the GRPR [22] were used in biological assays. Competition binding experiments with SB3 and [^{nat}Ga]SB3 were conducted in PC-3 cell membranes using [^{125}I-Tyr^4]BBN as the radioligand and [Tyr^4]BBN as reference (Supplementary material). In brief, the radioligand (~40,000 cpm per assay tube, at a 50 pM concentration) was incubated at 22 °C for 1 h and the assay conducted as previously reported [23]. IC_{50} values were calculated using nonlinear regression for a one-site model and represent mean±SD values from three independent experiments performed in triplicate.

The cell association of [^{67}Ga]SB3 in PC-3 cells was tested during a 1-h incubation period at 37 °C. Briefly, confluent PC-3 cells were seeded in six-well plates (~1.0×10^6 cells per well) 24 h before the experiment. Approximately 300,000 cpm of [^{67}Ga]SB3 (corresponding to 2 pmol total peptide in 150 μL of 0.5 % BSA/PBS supplemented with Haemaccel®) was added alone (total) or in the presence of 1 μM [Tyr^4]BBN (non-specific) and the experiment was performed as before [24]. Results were calculated as percentage internalized plus membrane bound activity versus total added activity per million cells.

Stability and biodistribution of [^{67}Ga]SB3 in mice

Blood collected 5 min pi of [^{67}Ga]SB3 in healthy mice was analyzed using high-performance liquid chromatography (HPLC) (Supplementary material).

For biodistribution studies, a≈150-μL bolus containing a suspension of≈1.5×10^7 freshly harvested human PC-3 cells in saline was subcutaneously injected into the flanks of female severe combined immunodeficiency (SCID) mice (15±3 g, 6 weeks of age on the day of arrival; NCSR "Demokritos" Animal House Facility). The animals were kept under aseptic conditions and 2–3 weeks later developed well-palpable tumors at the inoculation sites (80–150 mg). A 100-μL bolus (37 kBq, 10 pmol total peptide; in saline/EtOH 9/1 v/v) of [^{67}Ga]SB3 was injected into the tail vein and biodistribution was conducted for the 1-, 4-, and 24-h pi time intervals; for in

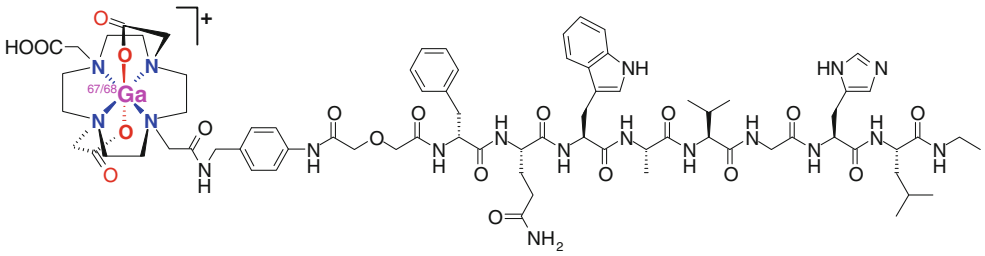

Fig. 1 Chemical structure of [$^{67/68}$Ga]SB3

vivo GRPR-blockade a separate 4-h animal group received excess [Tyr^4]BBN (40 nmol [Tyr^4]BBN in 50-μL vehicle coinjected with the radioligand). Biodistribution data were calculated as percentage injected dose per gram of tissue (%ID/g) with the aid of suitable standards for the injected dose [24].

Statistical analysis using the unpaired two-tailed Student's *t* test was performed to compare values between the control and the in vivo GRPR-blockade animal groups at 4 h pi; values of $P<0.05$ were considered statistically significant.

All animal experiments were carried out in compliance with European and national regulations and after approval of protocols by national authorities.

Patient selection and administration of [^{68}Ga]SB3

Seventeen patients (9 men and 8 women; age range, 40–74 years) with advanced PC or BC were iv injected with [^{68}Ga]SB3 (Table S1). The iv injection of [^{68}Ga]SB3 (mean administered activity of 283±91 MBq associated with a peptide mass of 23±0.7 nmol) was followed by the iv administration of furosemide (20 mg). Initial diagnosis using the classification of malignant tumors (TMN) was made using histopathology and tomography. All patients had had confirmed metastases to distant organs at last imaging and had demonstrated evident progression of tumor disease, e.g., a rise in tumor markers (PSA, CEA, Ca15-3 or CA-125) and/or progression on recent imaging (CT, MRI, and/or PET). Hematological (Hb, WBC, and platelets), liver (ALAT, AP, and γ-GT), and renal functions (s-creatinine and eGFR) were measured before [^{68}Ga]SB3 injection. Heart rate, blood pressure, and oxygenation were monitored throughout administration. Patients were asked to report side effects (dizziness, vomiting, abdominal discomfort) during injection and imaging. At the follow-up visits they were asked to report side effects. In three patients (numbers 4, 7, and 17) with recurrent PC an [^{18}F]fluoromethylcholine PET/CT scan was conducted. Written informed consent was obtained from all patients in accordance with German regulations for the administration of radiolabeled substances to humans. Data recording in a database was approved by all patients and by the local ethics committee.

Imaging protocol

All patients were scanned on a dual-modality PET/CT tomography scanner (Biograph duo; Siemens Medical Solutions). The CT component consists of a two-row spiral CT system and the PET component is based on a full-ring lutetium orthosilicate (LSO) PET system. Acquisition started 60–115 min pi. PC patients were requested to empty their bladder immediately before the PET/CT examination. They were positioned head first supine on the common patient handling system with the arms raised.

First, a topogram was acquired over 1,024 mm axially. Coaxial whole-body imaging ranges were defined on the topogram, covering an area from the skull to the upper thighs. CT was performed in spiral mode using a continuous acquisition at 130 kVp, 115 mAs, 4-mm collimation, 5-mm slice width, a table feed of 8 mm per rotation at 0.8-s rotation time, and 2.4-mm slice spacing. During the CT acquisition patients were asked to hold their breath in normal expiration. Three-dimensional PET emission scanning started in the caudocranial direction. An emission scan time of 2–3 min per bed position was used for all patients, with a total emission scan time of 24 min.

Data acquisition and interpretation

[^{68}Ga]SB3 scans were acquired from July 2009 until March 2010. After scatter and attenuation correction, PET emission data were reconstructed using an attenuation-weighted ordered subsets maximization expectation (OSEM) approach with two iterations, 8 subsets on 128×128 matrices and a 5-mm Gaussian postreconstruction filtering.

The CT images were evaluated on a Syngo viewing station by a skilled radiologist. Two experienced nuclear medicine physicians assessed the PET/CT images using E.soft (Syngo-based nuclear medicine software from Siemens Medical Solutions). Scintigraphic findings were compared with previous diagnostic examinations. [^{68}Ga]SB3 scans were defined as positive when focal, not physiological, accumulation of the radiotracer was found.

The maximum intensity projection (MIP) images were visually inspected and each single transversal slice was viewed from head to mid-thigh in combination with the CT image. Slice number and anatomical localization were recorded when

focal and abnormal tracer uptake was found. PET/CT fusion images were used for measurements of SUVmax in different organs/structures. Manually selected regions of interest (ROIs) were drawn on a single slice using the software provided by E.soft. SUVmax was calculated for the following organs: pancreas, kidney parenchyma, esophagogastric junction (EGJ), blood activity (blood pool), liver, lung, kidneys, and gluteus muscle.

Results

In vitro studies

Both SB3 and [^{nat}Ga]SB3 were able to displace [^{125}I-Tyr^4]BBN from GRPR sites on PC-3 membranes in a monophasic and dose-dependent manner (Fig. 2). Incorporation of Ga^{3+} favored receptor binding, as evident from the pertinent IC_{50} values of 4.6±0.4 nM (SB3) and 1.5±0.3 nM ([^{nat}Ga]SB3). During 1-h incubation of [^{67}Ga]SB3 with PC-3 cells at 37 °C, 22.2±1.2 % of added radioactivity remained on the cell membrane, with only 5.5±0.4 % detected within the cells, as consistent with an antagonist profile [19, 24]. In the presence of excess [Tyr^4]BBN, these values dropped to 1.5±0.1 % and 0.4± 0.1 % respectively, suggesting GRPR specificity.

Stability and biodistribution of [^{67}Ga]SB3 in mice

After entering the bloodstream of mice [^{67}Ga]SB3 remained >85 % stable, as revealed by HPLC analysis of blood samples collected 5 min pi (Fig. S3). This stability was found to be superior to previously reported values of GRPR-targeting radioligands [24–26].

The biodistribution of [^{67}Ga]SB3 in SCID mice bearing human PC-3 xenografts is shown in Fig. 3 for the 1-h, 4-h, and 24-h pi time points, with a separate 4-h animal group representing in vivo GRPR-blockade. The tracer rapidly cleared from blood, showing no retention in the kidneys. Likewise, background radioactivity declined with time, including GRPR-rich tissues, such as the mouse pancreas. In particular, the initially high pancreatic uptake of [^{67}Ga]SB3 at 1 h pi (≈160%ID/g) gradually dropped at the later time points (≥100%ID/g at 4 h and≈17%ID/g at 24 h pi), as consistent with a GRPR radioantagonist profile. Conversely, the uptake of [^{67}Ga]SB3 in the GRPR-positive xenografts remained remarkably high over time (33.1±3.9%ID/g at 1 h pi, 34± 6.9%ID/g at 4 h pi, and 27.1±0.9%ID/g at 24 h pi). Uptake in tumor and mouse pancreas was significantly reduced in the animals treated with excess [Tyr^4]BBN, confirming GRPR specificity.

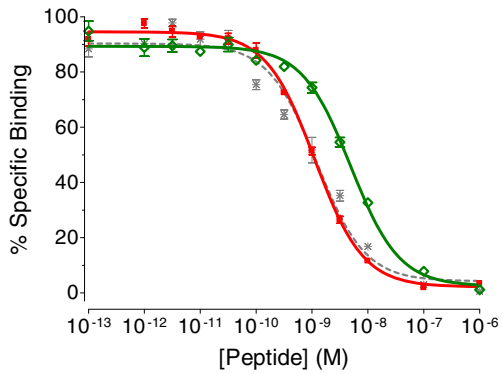

Fig. 2 Displacement of [^{125}I-Tyr^4]bombesin (BBN) from gastrin-releasing peptide receptor (GRPR) sites in PC-3 cell membranes by increasing concentrations of: ◇ SB3 (IC_{50}=4.6±0.4 nM); ■ [^{nat}Ga]SB3 (IC_{50}=1.5±0.3 nM); reference: ✳ [Tyr^4]BBN (IC_{50}=1.7±0.0.3 nM). Results represent the average IC_{50} values±SD of three independent experiments performed in triplicate

Safety, tolerability, and physiological distribution of [^{68}Ga]SB3 in patients

No local or systemic adverse effects were found. During injection, one patient had high blood pressure (RR 180/130), most likely due to anxiety. In this patient, diastolic and systolic pressure returned to normal levels within 1 h. The highest physiological uptake of [^{68}Ga]SB3 was found in the pancreas head (mean SUV 47.7). Mean SUVmax in the kidneys and at the EGJ was 5.4 and 3.3 respectively. High activity at the EGJ was previously described in preliminary clinical data with the GRPR agonist [^{68}Ga]AMBA [27]. An overview of the biodistribution is found in Fig. 4 (Table S2).

PET/CT results

A total of 71 lesions in 9 patients with positive [^{68}Ga]SB3 scans were recorded (Table S2). Mean SUVmax of these lesions in 9 patients was 4.2 (range 0.7–17.8). Thirty-eight lesions in group 1 (BC) were positive, with a median SUVmax of 2.0 (range 0.6–7.8). Thirty-three positive lesions in group 2 (PC) were positive, with a median SUVmax of 4.4 (range 1.7–17.8; Fig. 4; Tables S1–S3).

The characteristics of 8 BC and 9 PC patients injected with [^{68}Ga]SB3 are presented in Tables 1 and 2 respectively. Four BC patients (50 %) and 5 of the 9 PC patients (55 %) had positive lesions visualized by [^{68}Ga]SB3. Abnormal focal uptake on the [^{68}Ga]SB3 scan was seen in 2 patients. The first patient showed uptake on the left side in the supraspinatus muscle (SUVmax 2.2) and proximal adductor muscles (SUVmax 2.4), which was attributed to local shoulder inflammation. The second patient showed local uptake in the prostate (SUVmax 4.7), which was negative on other imaging modalities and attributed to calcifications in this tissue. One patient showed exceptionally high uptake on the [^{68}Ga]SB3 scan in several metastatic lymph nodes compared with the

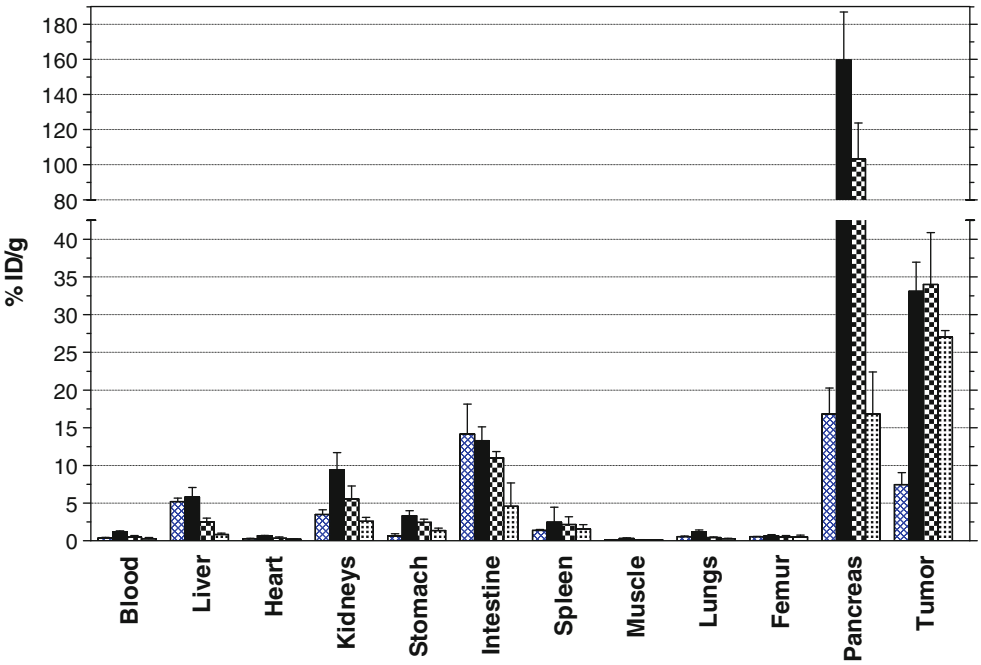

Fig. 3 Biodistribution of [^{67}Ga]SB3 in severe combined immunodeficiency (SCID) mice bearing human GRPR-positive PC-3 xenografts. Data are expressed as %ID/g and represent mean±SD, n=4, for ■ 1 h, ▩ 4 h and ▨ 24 h pi; ▨ a separate 4-h animal group represents in vivo GRPR-blockade.

follow-up scan performed with [^{18}F]fluoromethylcholine (Fig. 5).

The mean PSA level of PC patients was 64±81 ng/mL (range 1.5–215 ng/mL). Four out of 5 patients with a positive [^{68}Ga]SB3 scan had elevated PSA levels (≥10 ng/mL). One out of 4 patients with a negative [^{68}Ga]SB3 scan had normal PSA levels (Table 2).

Interestingly, osseous metastases could be well visualized in BC patients, as shown in Fig. 6 for patient number 6.

Discussion

The overexpression of GRPR in PC and BC offers promising opportunities for staging, monitoring, and potentially also for radionuclide therapy of these tumors with the application of

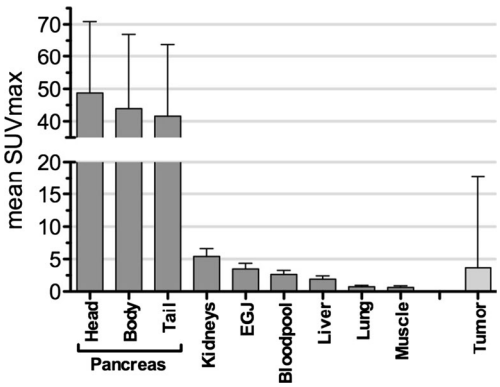

Fig. 4 SUVmax±SD in regions of interest (ROI) of [^{68}Ga]SB3 scans, including values for normal organs (n=17 patients) and for 71 [^{68}Ga]SB3-positive lesions in 9 patients

GRPR-specific radiopeptide probes [9, 10, 14, 17, 18]. A great number of GRPR-directed radioligands studied in the past two decades are analogs of BBN, displaying agonistic activity at the GRPR. While internalization of radiolabeled GRPR agonists was originally considered advantageous for in vivo tumor targeting, injection into patients was soon linked to undesirable pharmacological effects, raising biosafety concerns [21]. Recent studies on GRPR radioantagonists with better inherent biosafety have inadvertently brought to light their superior tumor targeting efficacy and faster background clearance compared with agonists. Based on the well-characterized GRPR antagonist, [^{99m}Tc]DB1 [19], we introduce here its DOTA-modified mimic, SB3, which can be labeled with ^{68}Ga (Fig. 1). We have thus designed a new ^{68}Ga-radiotracer suitable for PET and complementary to the existing SPECT radiotracer [^{99m}Tc]DB1. In addition, we have evaluated the novel PET radiotracer first in in vitro and animal GRPR-positive models and then in BC and PC patients, following an integrated "bench-to-patient" approach.

At the preclinical level, both SB3 and [^{nat}Ga]SB3 exhibited high affinity for the human GRPR expressed on PC-3 cells (Fig. 2). Moreover, [^{67}Ga]SB3 strongly and specifically bound onto the membrane of PC-3 cells, internalizing poorly, as expected for a GRPR-radioantagonist [19, 24]. Of great advantage is the stability of [^{67}Ga]SB3 in the mouse bloodstream (Fig. S3), favoring sufficient delivery to tumor sites, in contrast to the rapid in vivo catabolism previously reported for GRPR radioligands by neutral endopeptidase and possibly other enzymes [24, 26, 28]. High uptake of [^{67}Ga]SB3 was observed in PC xenografts in mice at 1 h pi (Fig. 3), which

Table 1 Characteristics and scan results in the subgroup of 8 breast cancer (*BC*) patients

Patient (number)	Age (years)	Final diagnosis	Initial stage	Year of diagnosis	Previous therapy	[^{68}Ga]SB3 scan
2	55	BC	T2N1M0	1999	Mast2, chem	+
3	70	BC LC	T1N2M1 Stage IV	1988 2008	Mast2, rad Chem	+
5	49	BC	T1N1M0	2001	Mast2, chem, rad, horm, sam, imm	+
6	48	BC	T1N0M0 T3N0M1	Left: 1998 Right: 2007	Mast2, chem, horm, rad, sam	+
8	60	BC	TxNxMx T1N0M0	Left: 1993 Right: 1999	Left: mast1 Right: mast1	−
9	51	BC	TxNxMx	1994	Mast2, chem, rad, imm	−
11	69	BC	T2N1M0	2004	Mast, chem, rad, imm	−
14	40	BC	T2N1M0	1999	Mast2, chem	−

mast1 mastectomy, *mast2* mastectomy plus lymphadenectomy, *chem* chemotherapy, *rad* external radiotherapy, *LC* lung cancer, *horm* anti-estrogen therapy, *sam* radioactive samarium, *imm* immunotherapy

remained at high levels up to 24 h pi. At the same time, values in the GRPR-rich mouse pancreas, although very high at the initial time points, declined rapidly over time. Likewise, background radioactivity cleared rapidly over time, leading to an attractive overall profile. On the other hand, the tumor uptake of [^{67}Ga]SB3 surpassed the values previously reported for [^{99m}Tc]DB1 in the same animal model at all time points [19]. Tumor retention in particular was clearly superior for [^{67}Ga]SB3 (27.1±0.9%ID/g) compared with [^{99m}Tc]DB1 (5.4±0.7%ID/g at 24 h pi).

This attractive preclinical profile prompted us to further evaluate [^{68}Ga]SB3 in a first-in-man study including a small number of PC and BC patients. Several pilot clinical studies with GRPR radioligands have been reported, including both PC and BC patients [13, 17, 21, 27]. However, most of these radioligands were BBN-based receptor agonists. A ^{64}Cu-labeled GRPR radioantagonist, ^{64}Cu-CB-TE2A-AR06 [(^{64}Cu-4,11-bis(carboxymethyl)-1,4,8,11-tetraazabicyclo(6.6.2)hexadecane)-PEG$_4$-D-Phe-Gln-Trp-Ala-Val-Gly-His-Sta-LeuNH$_2$], was recently studied in four patients with newly diagnosed PC using PET/CT. The radiotracer showed favorable tumor-to-normal organ ratios over time [29]. The most promising clinical results in 11 primary PC patients scheduled for radical prostatectomy were presented for the GRPR radioantagonist, [^{68}Ga]BAY86-7548 (^{68}Ga-DOTA-4-amino-1-carboxymethyl-piperidine-DPhe-Gln-Trp-Ala-Val-Gly-His-Sta-Leu-NH$_2$). Sensitivity and specificity of 88 % and 81 % were reported [30]. In the case of BC, no data have hitherto been provided on the diagnostic efficacy of a GRPR antagonist-based radioligand in patients. Good diagnostic sensitivity was demonstrated in early-stage BC patients during clinical evaluation of a series of ^{99m}Tc-radiotracers based on BBN, which were performed during the last decade [31–33]. In most of these studies, however, osseous involvement was not visualized, although the primary tumor and lymph node metastases were well visualized.

In the clinical part of our study, we have included patients with progressive disseminated disease for the evaluation of uptake in tumor metastases. For example, bone metastases were well visualized in patient number 6 with BC (Fig. 6), highlighting the promising imaging qualities of [^{68}Ga]SB3. As our patients have a long history of recurrent disease, other

Table 2 Characteristics and scan results in the subgroup of 9 prostate cancer (*PC*) patients

Patient (number)	Age (years)	Final diagnosis	Initial stage	Year of diagnosis	Previous therapy	PSA (ng/mL	[^{68}Ga]SB3 scan
1	59	PC	TxNxM1	2006	Rad, chem	89	+
4	74	PC	T1N0M0	2003	Horm, nephr, rad	40	+
7	70	PC	T4N1M0	2005	Prost, rad, horm, phos	182	+
10	70	PC	T3N1Mx	2002	Prost, rad, chem	215	+
12	53	PC	TxNxM1	2004	Lymph, horm	4	-
13	71	PC	T4N0M0	2001	Prost, horm	2	-
15	61	PC	T4NxM1	2006	Horm, rad, chem	32	-
16	54	PC	TxNxM1	2009	Horm, phos	7	-
17	69	PC	T3N0Mx	2004	Prost, rad	5	+

prost prostatectomy, *rad* radiotherapy, *chem* chemotherapy, *nephr* nephrectomy, *phos* bisphosphonates therapy, *horm* anti-androgen therapy

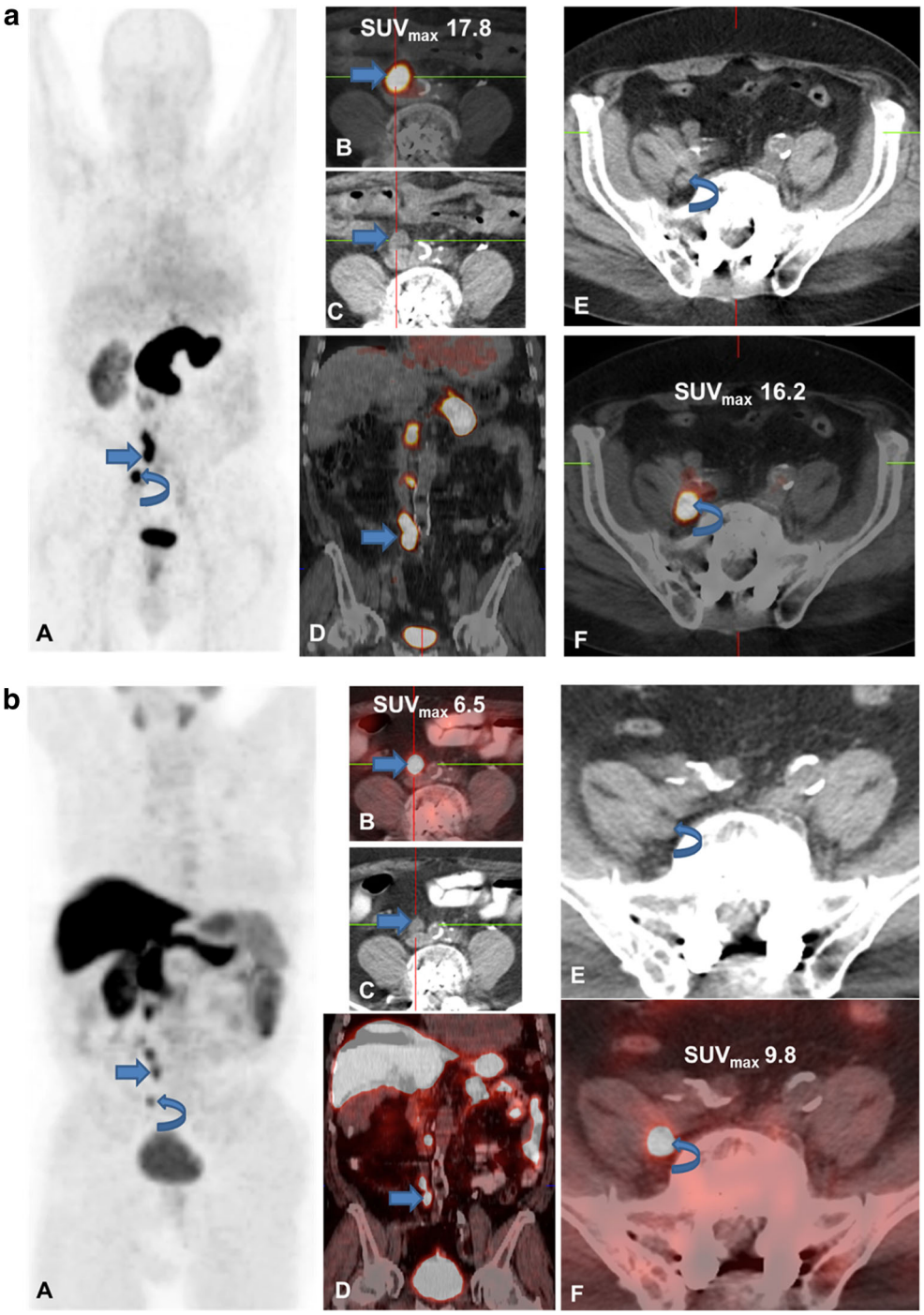

Fig. 5 **a** [^{68}Ga]SB3 PET/CT and **b** ^{18}F-choline PET/CT scan in a prostate cancer (PC) patient (number 4), demonstrating GRPR-positive and choline-avid lymph node metastases respectively: right to the aortic bifurcation (**B**–**D**, *straight arrow*) and right iliac lymph node metastasis at the level of the S1 vertebra (**E**, **F**, *curved arrow*). **A** MIP; **B**, **F** fused axial PET/CT images; **C**, **E** axial CT images; **D** fused coronal PET/CT image

(nuclear) imaging modalities were available and were additionally used for lesion detection. In one patient, [^{68}Ga]SB3 clearly demonstrated better performance in comparison with [^{18}F]fluoromethylcholine PET/CT (Fig. 5). However, the total number of positive [^{68}Ga]SB3 scans was lower compared with other studies, presumably as a result of recurrent, extensive disease history and previous therapies in our patients. It should be noted that GRPR is strongly upregulated in most of the primary prostate cancers that are still confined to the prostate, particularly in well-differentiated prostate tumors. On the other hand, a significant decline in GRPR expression is observed in the advanced androgen-independent stages of PC [9, 10, 12]. Recently, an inverse correlation was reported between GRPR expression vs high PSA values and high Gleason score [11]. Results were obtained from screening multiple prostate samples for GRPR expression in 530 patients, with most of the primary carcinoma specimens (77 %) acquired after radical prostatectomy. For BC, GRPR

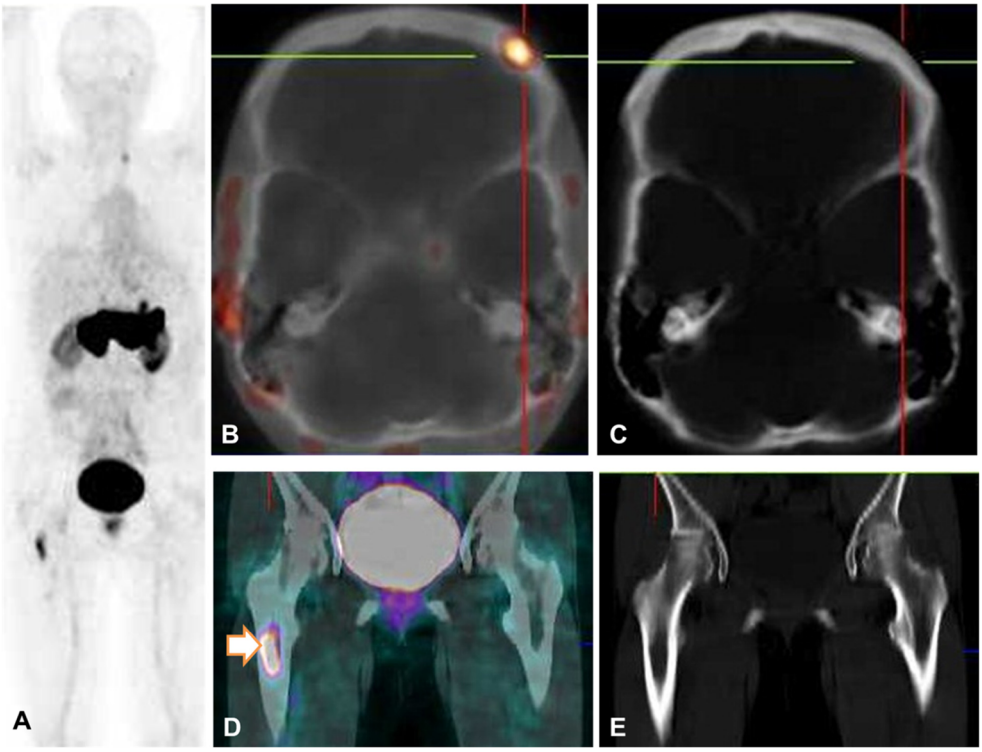

Fig. 6 [^{68}Ga]SB3 scan in a breast cancer (BC) patient (number 6), demonstrating GRPR-positive bone metastasis in the skull: frontal bone on the left side (**B**, SUV_{max} 2.4) and bone marrow metastasis in the right proximal femur (**D**, *arrow*, SUV_{max} 7.8), both negative on CT (**C**, **E**). **A** MIP; **B** fused axial PET/CT image; **C**, **E** axial CT images; **D** fused coronal PET/CT image

expression has been correlated with estrogen receptor levels [16, 34].

Despite the fact that all patients in our study had disseminated recurrent disease and many had a history of previous therapies, including anti-hormonal therapy, potentially leading to a state of androgen/estrogen independence and consequently to a higher number of negative scans with [^{68}Ga]SB3, we still found positive scans in about 50 % of cases, both in BC and in PC. This indicates the potential value of GRPR as a biomarker for monitoring after therapy. A preclinical study in nude mice with xenografted BC did indeed demonstrate better visualization and monitoring of hormone treatment with the bombesin agonist ^{68}Ga-AMBA vs ^{18}F-FDG [35]. It is reasonable to assume that a higher number of [^{68}Ga]SB3 scans would have been positive in early BC and PC cases. This hypothesis is currently under investigation in a clinical study in patients with primary PC initiated at Erasmus MC.

The benefit of choline PET/CT was recently shown in the preoperative staging of PC patients with an intermediate or high risk of extracapsular disease, leading to a different therapeutic treatment in 19 out of 130 patients (15 %) [36]. [^{68}Ga]SB3 could be used in addition to conventional imaging for upstaging nearby lymph nodes and/or distant metastases. In patients with local recurrent PC, choline PET/CT can be used to delineate local sites of recurrence. However, irradiation planning for the treatment of single lymph node metastases on the basis of choline PET/CT remains controversial owing to its limited lesion-based sensitivity in primary nodal staging [37]. Furthermore, the detection rate of choline-PET/CT is poor in patients with low PSA levels (<3.0 ng/ml) [37]. PET/CT with [^{68}Ga]SB3 may be valuable in this group of PC patients and could improve radiation treatment planning by enhancing the target volume to, for example, lymphatic drainage sites.

Prostate-specific membrane antigen (PSMA) is another interesting target for imaging. PSMA is expressed in normal and malignant prostatic epithelium with high expression in poorly differentiated metastatic carcinomas [38, 39]. Small molecule PSMA inhibitors demonstrated good imaging characteristics in patients with androgen-independent PC with bone metastasis, but have a lower sensitivity in patients with primary PC [40]. GRPR expression, on the other hand, is higher in the early stages of PC, in contrast to PSMA (Fig. 7). A comparative study of [^{68}Ga]SB3 and a PSMA-targeted PET radiotracer in patients with primary or recurrent PC would therefore be of utmost interest for further evaluation and clinical use.

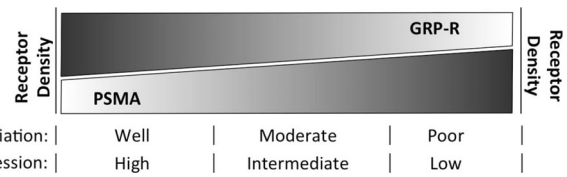

Fig. 7 Graphical representation of imaging characteristics for gastrin-releasing peptide receptor (*GRPR*) and prostate-specific membrane antigen (*PSMA*) in PC as a function of histological differentiation grade and androgen receptor (*AR*) expression

Conclusion

We introduce here a new GRPR antagonist suitable for labeling with ^{68}Ga. Preclinical experience with the [^{67}Ga]SB3 surrogate revealed the most attractive radiotracer qualities, such as high GRPR-affinity, good in vivo stability, and excellent targeting efficacy in human GRPR-positive xenografts in mice. First clinical data with [^{68}Ga]SB3 PET/CT in patients with disseminated PC and BC showed encouraging results, as lesions were visualized in about 50 % of the patients, despite their advanced disease. The number of positive [^{68}Ga]SB3 scans is expected to be higher in patients with primary PC and BC. This prospect favors the application of [^{68}Ga]SB3 as an attractive tool for PC and BC staging, monitoring, and eventually patient stratification for radionuclide therapy with [^{177}Lu/^{90}Y/^{213}Bi]SB3.

Compliance with ethical standards

Conflicts of interest None.

Ethical approval All applicable international, national, and/or institutional guidelines for the care and use of animals were followed.

All procedures performed in studies involving human participants were in accordance with the ethical standards of the institutional and/or national research committee and with the 1964 Declaration of Helsinki and its later amendments or comparable ethical standards.

Informed consent Informed consent was obtained from all individual participants included in the study.

Glossary

[^{99m}Tc]DB1	^{99m}Tc-(N′$_4$)-DPhe-Gln-Trp-Ala-Val-Gly-His-Leu-NHEt)
[^{99m}Tc]DB4	^{99m}Tc-N$_4$-Pro-Gln-Arg-Tyr-Gly-Asn-Gln-Trp-Ala-Val-Gly-His-Leu-Nle-NH$_2$
DOTA	1,4,7,10-tetraazacyclododecane-1,4,7,10-tetraacetic acid

References

1. Siegel R, Naishadham D, Jemal A. Cancer statistics, 2012. CA Cancer J Clin. 2012;62:10–29. doi:10.3322/caac.20138.
2. DeSantis C, Siegel R, Bandi P, Jemal A. Breast cancer statistics, 2011. CA Cancer J Clin. 2011;61:409–18. doi:10.3322/caac.20134.
3. Roehl KA, Antenor JA, Catalona WJ. Serial biopsy results in prostate cancer screening study. J Urol. 2002;167:2435–9.
4. Elter M, Schulz-Wendtland R, Wittenberg T. The prediction of breast cancer biopsy outcomes using two CAD approaches that both emphasize an intelligible decision process. Med Phys. 2007;34:4164–72.
5. Hricak H, Choyke PL, Eberhardt SC, Leibel SA, Scardino PT. Imaging prostate cancer: a multidisciplinary perspective. Radiology. 2007;243:28–53. doi:10.1148/radiol.2431030580.
6. Berg WA, Gutierrez L, NessAiver MS, Carter WB, Bhargavan M, Lewis RS, et al. Diagnostic accuracy of mammography, clinical examination, US, and MR imaging in preoperative assessment of breast cancer. Radiology. 2004;233:830–49. doi:10.1148/radiol.2333031484.
7. Jadvar H. Imaging evaluation of prostate cancer with ^{18}F-fluorodeoxyglucose PET/CT: utility and limitations. Eur J Nucl Med Mol Imaging. 2013;40 (Suppl 1):S5–10. doi:10.1007/s00259-013-2361-7.
8. Escalona S, Blasco JA, Reza MM, Andradas E, Gomez N. A systematic review of FDG-PET in breast cancer. Med Oncol. 2010;27:114–29. doi:10.1007/s12032-009-9182-3.
9. Markwalder R, Reubi JC. Gastrin-releasing peptide receptors in the human prostate: relation to neoplastic transformation. Cancer Res. 1999;59:1152–9.
10. Körner M, Waser B, Rehmann R, Reubi JC. Early over-expression of GRP receptors in prostatic carcinogenesis. Prostate. 2014;74:217–24. doi:10.1002/pros.22743.
11. Beer M, Montani M, Gerhardt J, Wild PJ, Hany TF, Hermanns T, et al. Profiling gastrin-releasing peptide receptor in prostate tissues: clinical implications and molecular correlates. Prostate. 2012;72:318–25. doi:10.1002/pros.21434.
12. Schroeder RP, de Visser M, van Weerden WM, de Ridder CM, Reneman S, Melis M, et al. Androgen-regulated gastrin-releasing peptide receptor expression in androgen-dependent human prostate tumor xenografts. Int J Cancer. 2010;126:2826–34. doi:10.1002/ijc.25000.
13. Mather SJ, Nock BA, Maina T, Gibson V, Ellison D, Murray I, et al. GRP receptor imaging of prostate cancer using [^{99m}Tc]Demobesin 4: a first-in-man study. Mol Imaging Biol. 2014;16:888–95. doi:10.1007/s11307-014-0754-z.
14. Gugger M, Reubi JC. Gastrin-releasing peptide receptors in non-neoplastic and neoplastic human breast. Am J Pathol. 1999;155:2067–76. doi:10.1016/S0002-9440(10)65525-3.
15. Reubi C, Gugger M, Waser B. Co-expressed peptide receptors in breast cancer as a molecular basis for in vivo multireceptor tumour targeting. Eur J Nucl Med Mol Imaging. 2002;29:855–62. doi:10.1007/s00259-002-0794-5.
16. Halmos G, Wittliff JL, Schally AV. Characterization of bombesin/gastrin-releasing peptide receptors in human breast cancer and their relationship to steroid receptor expression. Cancer Res. 1995;55:280–7.
17. Maina T, Nock B, Mather S. Targeting prostate cancer with radiolabelled bombesins. Cancer Imaging. 2006;6:153–7. doi:10.1102/1470-7330.2006.0025.
18. Yu Z, Ananias HJ, Carlucci G, Hoving HD, Helfrich W, Dierckx RA, et al. An update of radiolabeled bombesin analogs for gastrin-releasing peptide receptor targeting. Curr Pharm Des. 2013;19:3329–41.
19. Cescato R, Maina T, Nock B, Nikolopoulou A, Charalambidis D, Piccand V, et al. Bombesin receptor antagonists may be preferable to agonists for tumor targeting. J Nucl Med. 2008;49:318–26. doi:10.2967/jnumed.107.045054.
20. Mansi R, Wang X, Forrer F, Kneifel S, Tamma ML, Waser B, et al. Evaluation of a 1,4,7,10-tetraazacyclododecane-1,4,7,10-tetraacetic acid-conjugated bombesin-based radioantagonist for the labeling with single-photon emission computed tomography, positron emission tomography, and therapeutic radionuclides. Clin Cancer Res. 2009;15:5240–9. doi:10.1158/1078-0432.CCR-08-3145.
21. Bodei L, Ferrari M, Nunn A, Llull J, Cremonesi M, Martano L, et al. ^{177}Lu-AMBA bombesin analogue in hormone refractory prostate cancer patients: a phase I escalation study with single-cycle administrations. Eur J Nucl Med Mol Imaging. 2007;34:S221.
22. Reile H, Armatis PE, Schally AV. Characterization of high-affinity receptors for bombesin/gastrin releasing peptide on the human prostate cancer cell lines PC-3 and DU-145: internalization of receptor bound ^{125}I-(Tyr^4)bombesin by tumor cells. Prostate. 1994;25:29–38.

23. Nock BA, Nikolopoulou A, Galanis A, Cordopatis P, Waser B, Reubi JC, et al. Potent bombesin-like peptides for GRP-receptor targeting of tumors with ^{99m}Tc: a preclinical study. J Med Chem. 2005;48:100–10. doi:10.1021/jm049437y.
24. Marsouvanidis PJ, Nock BA, Hajjaj B, Fehrentz JA, Brunel L, M'Kadmi C, et al. Gastrin releasing peptide receptor-directed radioligands based on a bombesin antagonist: synthesis, ^{111}In-labeling, and preclinical profile. J Med Chem. 2013;56:2374–84. doi:10.1021/jm301692p.
25. Marsouvanidis PJ, Maina T, Sallegger W, Krenning EP, de Jong M, Nock BA. Tumor diagnosis with new ^{111}In-radioligands based on truncated human gastrin releasing peptide sequences: synthesis and preclinical comparison. J Med Chem. 2013;56:8579–87. doi:10.1021/jm4010237.
26. Nock BA, Maina T, Krenning EP, de Jong M. "To serve and protect": enzyme inhibitors as radiopeptide escorts promote tumor targeting. J Nucl Med. 2014;55:121–7. doi:10.2967/jnumed.113.129411.
27. Baum RP, Prasad V, Frischknecht M, Maecke H, Reubi J. Bombesin receptor imaging in various tumors: first results of Ga-68 AMBA PET/CT. Eur J Nucl Med Mol Imaging. 2007;34:S193-S.
28. Linder KE, Metcalfe E, Arunachalam T, Chen J, Eaton SM, Feng W, et al. In vitro and in vivo metabolism of Lu-AMBA, a GRP-receptor binding compound, and the synthesis and characterization of its metabolites. Bioconjug Chem. 2009;20:1171–8. doi:10.1021/bc9000189.
29. Wieser G, Mansi R, Grosu AL, Schultze-Seemann W, Dumont-Walter RA, Meyer PT, et al. Positron emission tomography (PET) imaging of prostate cancer with a gastrin releasing peptide receptor antagonist—from mice to men. Theranostics. 2014;4:412–9. doi:10.7150/thno.7324.
30. Kähkönen E, Jambor I, Kemppainen J, Lehtio K, Gronroos TJ, Kuisma A, et al. In vivo imaging of prostate cancer using [^{68}Ga]-labeled bombesin analog BAY86-7548. Clin Cancer Res. 2013;19:5434–43. doi:10.1158/1078-0432.CCR-12-3490.
31. Van de Wiele C, Phonteyne P, Pauwels P, Goethals I, Van den Broecke R, Cocquyt V, et al. Gastrin-releasing peptide receptor imaging in human breast carcinoma versus immunohistochemistry. J Nucl Med. 2008;49:260–4. doi:10.2967/jnumed.107.047167.
32. Shariati F, Aryana K, Fattahi A, Forghani MN, Azarian A, Zakavi SR, et al. Diagnostic value of ^{99m}Tc-bombesin scintigraphy for differentiation of malignant from benign breast lesions. Nucl Med Commun. 2014;35:620–5. doi:10.1097/MNM.0000000000000112.
33. Scopinaro F, Di Santo GP, Tofani A, Massari R, Trotta C, Ragone M, et al. Fast cancer uptake of ^{99m}Tc-labelled bombesin (^{99m}Tc BN1). In Vivo. 2005;19:1071–6.
34. Dalm SU, Martens JW, Sieuwerts AM, van Deurzen CH, Koelewijn SJ, de Blois E, et al. In-vitro and in-vivo application of radiolabeled gastrin releasing peptide receptor ligands in breast cancer. J Nucl Med. 2015;56:752–7. doi:10.2967/jnumed.114.153023.
35. Prignon A, Nataf V, Provost C, Cagnolini A, Montravers F, Gruaz-Guyon A, et al. ^{68}Ga-AMBA and ^{18}F-FDG for preclinical PET imaging of breast cancer: effect of tamoxifen treatment on tracer uptake by tumor. Nucl Med Biol. 2015;42:92–8. doi:10.1016/j.nucmedbio.2014.10.003.
36. Beheshti M, Imamovic L, Broinger G, Vali R, Waldenberger P, Stoiber F, et al. ^{18}F choline PET/CT in the preoperative staging of prostate cancer in patients with intermediate or high risk of extracapsular disease: a prospective study of 130 patients. Radiology. 2010;254:925–33. doi:10.1148/radiol.09090413.
37. Kitajima K, Murphy RC, Nathan MA. Choline PET/CT for imaging prostate cancer: an update. Ann Nucl Med. 2013;27:581–91. doi:10.1007/s12149-013-0731-7.
38. Silver DA, Pellicer I, Fair WR, Heston WD, Cordon-Cardo C. Prostate-specific membrane antigen expression in normal and malignant human tissues. Clin Cancer Res. 1997;3:81–5.
39. Wright Jr GL, Grob BM, Haley C, Grossman K, Newhall K, Petrylak D, et al. Upregulation of prostate-specific membrane antigen after androgen-deprivation therapy. Urology. 1996;48:326–34.
40. Ristau BT, O'Keefe DS, Bacich DJ. The prostate-specific membrane antigen: lessons and current clinical implications from 20 years of research. Urol Oncol. 2014;32:272–9. doi:10.1016/j.urolonc.2013.09.003.